Chaotic phase synchronization in scale-free networks of bursting neurons

C. A. S. Batista,[1] A. M. Batista,[1] J. A. C. de Pontes,[2] R. L. Viana,[2,*] and S. R. Lopes[2]
[1]*Departamento de Matemática e Estatística, Universidade Estadual de Ponta Grossa, 84032-900 Ponta Grossa, Paraná, Brazil*
[2]*Departamento de Física, Universidade Federal do Paraná, 81531-990 Curitiba, Paraná, Brazil*
(Received 30 November 2006; revised manuscript received 16 May 2007; published 30 July 2007)

There is experimental evidence that the neuronal network in some areas of the brain cortex presents the scale-free property, i.e., the neuron connectivity is distributed according to a power law, such that neurons are more likely to couple with other already well-connected ones. From the information processing point of view, it is relevant that neuron bursting activity be synchronized in some weak sense. A coherent output of coupled neurons in a network can be described through the chaotic phase synchronization of their bursting activity. We investigated this phenomenon using a two-dimensional map to describe neurons with spiking-bursting activity in a scale-free network, in particular the dependence of the chaotic phase synchronization on the coupling properties of the network as well as its synchronization with an externally applied time-periodic signal.

DOI: 10.1103/PhysRevE.76.016218 PACS number(s): 05.45.Xt, 87.19.La

I. INTRODUCTION

A biological neuron is a unit of a large system, the brain, consisting of about a hundred specialized modules with different functions, each of them being a complex network itself, where each neuron receives excitatory inputs from a few thousands of other neurons [1]. Neuronal activity (i.e., the evolution of the action potential) in cortical circuits often presents two distinct time scales: (i) a fast time scale characterized by repetitive spiking; and (ii) a slow time scale with bursting activity, where neuron activity alternates between a quiescent state and spiking trains [2]. A characteristic feature of cortical circuits is that they produce common rhythmic bursting, while its individual neurons, when isolated, show irregular bursts [3]. Many mathematical models emulate this spiking-bursting behavior, ranging from differential equations [4] to discrete-time maps [5,6].

Interacting bursting neurons can exhibit basically two types of common rhythmic bursting: synchronization of bursts, where the neurons burst at the same time, regardless of the further evolution of their spikes; and complete synchronization, which involves also synchronization of spikes [2]. There follows that burst synchronization is weaker than complete synchronization and thus easier to achieve, in terms of the coupling strength needed. The existence of a slow time scale in coupled bursting neurons enables us to define a bursting phase and frequency (its time rate) for each of them, even though on the spiking time scale they behave asynchronously [7]. From this point of view, the existence of coherent bursting may be regarded as an example of chaotic phase synchronization, which is a widely investigated phenomenon in a variety of physical and biological systems [8]. Chaotic phase synchronization is defined as the occurrence of a certain relation between phases of interacting systems, bursting neurons in our case, while the amplitudes (related to the spiking time scales) can remain chaotic and uncorrelated [9].

The transition to mutual chaotic phase synchronization in bursting neurons was shown to occur as the coupling strength is large enough, for a global coupling scheme where each neuron interacts with the mean field produced by the network [7]. This problem has been studied in the context of a complete synchronization of neuron activity, and the onset of synchronization was found to depend only on the number of connections received by each neuron, provided this number is the same for all neurons, regardless of other details of the network [2]. For chaotic phase synchronization, however, there remains open the question of how the transition to synchronized bursting depends on network properties, as the coupling topology and strength.

Recent experimental evidence suggests that some brain activities can be assigned to scale-free networks, as revealed by functional magnetic resonance imaging [10]. In scale-free networks the number k of connections *per* neuron satisfies a power-law probability distribution $P(k) \sim k^{-\varpi}$, in such a way that highly connected neurons are connected, on the average, with highly connected ones, a property also found in many social and computer networks [11,12]. The scaling exponent ϖ has been found to take on values between 2.0 and 2.2, with an average number of connections $\langle k \rangle \approx 4$ per neuron [10]. This topology is consistent with the fact that the brain network increases its size by the addition of new neurons, and the latter attach preferentially to already well-connected neurons [1].

Scale-free networks appear in a wide variety of situations, as in the World Wide Web [13], earthquakes [14], large computer programs [15], epidemic spreading [16], human sexual contacts [17], protein domain distributions [18], and cellular metabolic chains [19], just to mention a few representative examples. The peculiar coupling topology exhibited by scale-free networks makes them easier to synchronize than some types of regular lattices [20,21]. We have found that this also occurs for a weaker form of synchronization called direction coherence (a discrete-time analog of phase synchronization) in coupled chaotic maps [22]. Chou and Kurths have observed an interesting property of scale-free networks with prospective applications for neuronal lattices: when complete synchronization is achieved in such lattices, the coupling strength becomes weighted and correlated with the topology due to a hierarchical transition to synchronization

*Corresponding author. viana@fisica.ufpr.br

in heterogeneous networks [23]. The use of a scale-free lattice does not necessarily imply that the shortcuts connect distant neurons, since the physical distance among neurons does not play any role in the scale-free model we have used. Hence our model can describe electrical synapses, where the coupling can only exist between neighboring neurons [24,25]. Chemical synapses, on the other hand, would need an on-off threshold in order to model neuron excitability [5,26].

In this paper we investigate the onset of chaotic phase synchronization of bursting neurons modeled by a network of coupled two-dimensional maps exhibiting the scale-free property. Since neuronal networks are embedded in a three-dimensional lattice in the brain, where the nodes are the neurons, connected by axons and dendrites, we use a coupled map lattice possessing a power-law connectivity per neuron with exponent $\varpi=2.08$, compatible with the networks described in Refs. [10]. We use some numerical diagnostics related to the time evolution of the bursting phases and their time rates to characterize the transition to a phase synchronized state. Such a transition is found to be dependent on the coupling strength as well as on properties of the coupling scheme used in the obtention of the scale-free lattice. Moreover, we analyze the synchronization of the neuron bursting evolution with an externally applied harmonic signal, which has been proposed as an electrical stimulation of the brain to suppress undesirable rhythms related to pathologies [27].

The remainder of this paper is organized as follows: in Sec. II we present the properties of the map describing neuron dynamics, as well as the definition of a geometrical phase for the bursting dynamics. Sec. III describes the obtention of a scale-free lattice and some of its properties. Section IV deals with the dependence of chaotic phase synchronization on the network properties using suitable numerical diagnostics. In Sec. V we consider the synchronization between the bursting phases of neurons and the driving phase provided by a time-periodic external signal applied to one selected neuron. Our conclusions are left to the last section.

II. NEURON DYNAMICS AND PHASE SYNCHRONIZATION

Bursting neurons present two time scales, since there is a slow process (bursting) modulating the fast action-potential firing (spiking) [28]. The emergence of such multiple time scales is only possible in neuron models consisting of three or more ordinary differential equations, like the Hindmarch-Rose model [4]. A further simplification is obtained by using discrete-time systems, and the simpler maps with this property are two-dimensional, like the model proposed by Rulkov [6]

$$x_{n+1} = \frac{\alpha}{1+x_n^2} + y_n, \tag{1}$$

$$y_{n+1} = y_n - \sigma x_n + \beta, \tag{2}$$

where x_n is the fast and y_n is the slow dynamical variable. The first variable has a dynamical behavior emulating the spiking-bursting activity of a neuron, depending on the parameter α, whereas the latter variable undergoes a slow evolution because of the small values taken on by the parameters σ and β, which model the action of external dc bias current and synaptic inputs on a given isolated neuron [29].

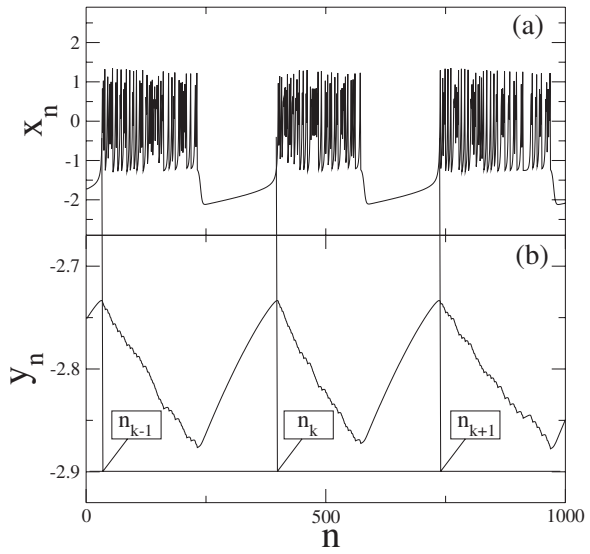

FIG. 1. Time evolution of the (a) fast and (b) slow variables in the Rulkov map (1) and (2) for $\alpha=4.1$, $\sigma=\beta=0.001$, showing the times sampled to define a bursting phase.

The parameter α is selected within the range [4.1,4.4], for which the map (1) and (2) yields chaotic dynamics for the fast variable x_n with the different time scales [Fig. 1(a)]. When considering assemblies of neurons we assign slightly different values of α for each map within this interval, taking into account the naturally occurring diversity of neuron cells. However, for such parameter values the uncoupled maps may produce either chaotic burst or simply continuous chaotic spiking, dependent on α. This reinforces the necessity of neuron coupling to produce a coherent neuron bursting activity in such inhomogeneous networks.

The emergence of bursting in the map (1) and (2) can be understood by using a simplified description of its dynamics. Since y_n is always a small input from slow dynamics we can approximate it by a constant γ and consider the one-dimensional resulting map, which has generally three fixed points $x^*_{1,2,3}$ such that the first two undergo a saddle-node bifurcation as γ approaches a critical value γ^* [6]. When $\gamma \gtrsim \gamma^*$ the fixed points $x^*_{1,2}$ disappear and a narrow channel forms between the map function and the 45° line, such that the fast variable displays chaotic oscillations corresponding to the spikes within a given burst. The end of the burst, on the other hand, is due to an external crisis of the chaotic attractor.

Unlike the bursting behavior exhibited by the fast variable, the slow variable y_n presents nearly regular saw-tooth oscillations, which will turn to be useful in order to define a bursting phase [Fig. 1(b)]. A burst is considered to begin when the slow variable has a local maximum, in well-defined instants of time we call n_k. The duration of the chaotic burst, $n_{k+1}-n_k$, depends on the variable x_n and fluctuates in an irregular fashion when x_n undergoes chaotic evolution. Never-

theless, we can define a phase describing the time evolution within each burst and varying from 0 to 2π as n evolves from n_k to n_{k+1}:

$$\varphi(n) = 2\pi k + 2\pi \frac{n - n_k}{n_{k+1} - n_k}, \tag{3}$$

and, since $n_{k+1} - n_k$ is different for each burst, there follows that the bursting phase rate also varies with time, such that we must look at the bursting frequency defined by

$$\Omega = \lim_{n \to \infty} \frac{\varphi(n) - \varphi(0)}{n}. \tag{4}$$

If the neurons are not coupled whatsoever, they can burst at different times yielding a typically noncoherent output. Their coupling, on the other hand, can force them to burst at roughly the same instant. Rigorous equality of bursting times cannot be achieved in a heterogeneous lattice since the interburst intervals $n_{k+1} - n_k$ are different in general. However, the outstanding feature of chaotic phase synchronization is that the phases can mutually adjust themselves, while the amplitudes remain uncorrelated. Hence in two phase synchronized neurons the times at which they burst are close, but their spiking activity is poorly or not correlated at all.

III. SCALE-FREE FUNCTIONAL BRAIN NETWORKS

From now on, we will consider an assembly of N neurons, each of them being described by the map (1) and (2). Many problems involving neural networks may be treated from the graph-theoretical point of view, such that the Euclidean distance between neurons does not play a significant role [30]. However, since biological neurons are embedded in a three-dimensional lattice in the brain, connected by axons and dendrites, it turns out to be more convenient to use a coupled map lattice embedded in a Euclidean space [31].

Coupled map lattices are paradigmatic models for a great variety of complex systems, presenting both space and time as discrete variables, while retaining a continuous state variable capable to undergo a smooth nonlinear dynamics [32]. Many theoretical studies of neural networks use coupled map lattices as models [33], due to some advantages like the need of less computer time in comparison with lattices of differential equations, which is particularly important if the required simulation requires the number of neurons N to be large.

We examine, in particular, a one-dimensional chain of N coupled maps of the form (1) and (2), where $(x_n^{(i)}, y_n^{(i)})$ represents the fast and slow variables for the neuron $i (i = 1, 2, \ldots N)$ at time n:

$$x_{n+1}^{(i)} = \frac{\alpha^{(i)}}{1 + (x_n^{(i)})^2} + y_n^{(i)} + \mathcal{C}^{(i)}(x_n^{(j)}, y_n^{(j)}) \quad (j \neq i), \tag{5}$$

$$y_{n+1}^{(i)} = y_n^{(i)} - \sigma^{(i)} x_n^{(i)} + \beta^{(i)}, \tag{6}$$

where we consider the case where all map parameters can be different for each site, and the coupling is performed only on the fast time scale by means of the term $\mathcal{C}^{(i)}$, the form of which depends on the network topology chosen to describe the neural network.

The latter is a question of paramount importance in the modeling of neuron assemblies in the brain. For example, the cerebral cortex has approximately $N = 10^{10}$ neurons, each of them receiving excitatory inputs from a few thousand of other neurons [10]. When the degree of connectivity, i.e., the average number of connections per neuron $\langle k \rangle$, is large enough, a global type of coupling has been usually chosen,

$$\mathcal{C}^{(i)}(x_n^{(i)}) = \frac{\epsilon}{N} \sum_{j=1}^{N} x_n^{(j)}, \tag{7}$$

where each neuron is coupled to the "mean field" generated by the entire lattice. This form of coupling has been extensively used in studies of synchronization of bursting neurons [6,7]. However, since such a description does not take into account the dependence of the coupling on the distance between neurons, and the connectivity is the same for all neurons ($\langle k \rangle = N$), the global coupling can only be considered a simplified model.

More realistic models of brain networks are quite difficult to build since networks of individual neurons are known for a limited number of cases only, as for the worm *C. elegans*, for which $N = 282$ and $\langle k \rangle = 14$ [34]. We usually have data from networks formed by neuron clusters (i.e., interrelation of functions related to cortical regions), detailed studies being available for the cortico-cortical network of cats [35] and macaques [36]. Other studies have considered the functional networks obtained through functional magnetic resonance imaging in humans, where the functional connections are defined from the correlation properties of their time evolution, and for which $N = 4891$ and $\langle k \rangle = 4.12$ [10].

A common property emerging from such complex neuron networks is that the connectivity is nonuniform, presenting a small number of highly connected neurons, while most of them remain poorly connected. In order to quantify the connection properties of the lattices there are two quantities of interest: (i) the shortest path length L, defined as the minimum number of links necessary to connect two nodes; and (ii) the clustering coefficient C, or the fraction of connections between the neighbors with respect to maximum possible. Regular lattices connecting only near neighbors display a relatively large amount of clustering C, but they fail to provide nonlocal interactions, which accounts for a large average distance L. Random graphs, on the other hand, have a substantially smaller value for L due to the randomly distributed nonlocal interactions, but they possess low values of the clustering coefficient C due to the sparseness of the connectivity among sites.

In the human functional network the shortest path length was found to be $L = 6.0$, with a cluster coefficient of $C = 0.15$ [10]. If this network were to be treated as a random graph, these quantities would take on the values $L_{random} = 6.0$ and $C_{random} = 0.000\,89$. Hence a more realistic network topology should be between the limiting cases of a regular (globally coupled) and a random lattices. Such a network exhibits the so-called *small-world* property, for it has a small value of L (just like in a random graph) while retaining a

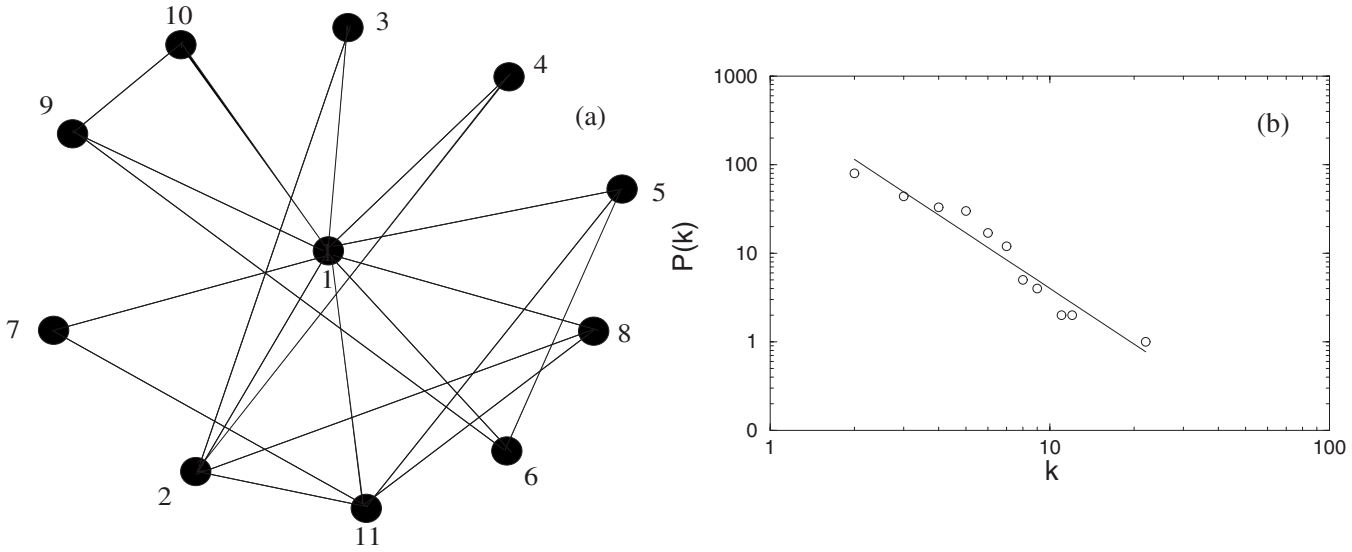

FIG. 2. (a) Scheme of the initial lattice with $N_0=11$ sites used to build a scale-free lattice. (b) Probability distribution for the connectivity of the final scale-free lattice with $N=230$ sites. The solid line is a least-squares fit with slope −2.08.

comparatively large clustering, as it occurs for regular lattices. Both properties can be achieved simultaneously through introducing random shortcuts into an otherwise purely regular lattice [37,38].

Besides having the small-world property, the human functional network is also characterized by a highly nonhomogeneous distribution characteristic of a *scale-free* network, for which the number of connections *per* node presents a statistical power-law dependence [11]. If $P(k)dk$ denotes the probability of finding a node with connectivity between k and $k+dk$, for scale-free lattices one has $P(k)\sim k^{-\varpi}$ where $\varpi>1$. This power-law distribution of connectivities is regarded as a consequence of two generic mechanisms [11]: networks expand continuously by the addition of new nodes and new nodes attach preferentially to already well-connected nodes. Chialvo and co-workers have shown that the connectivity distribution of the human functional network satisfies the scale-free scaling with an exponent ϖ between 2.0 and 2.2 [10]. By way of contrast, the macaque cortico-cortical network fails to present the scale-free property, maybe due to the smallness of the network size, a problem also observed for the cat network [39].

In this paper we use the Barabási-Albert coupling prescription to generate scale-free lattice of the form (5) and (6), where the coupling term is

$$\mathcal{C}^{(i)}(x_n^{(i)}) = \frac{\epsilon}{k^{(i)}} \sum_{j\in I} x_n^{(j)}, \tag{8}$$

where $\epsilon>0$ is the coupling strength and we assumed that each site i is coupled with a set I comprising $k^{(i)}$ other sites randomly chosen along the lattice according to the procedure to be explained below. We use free boundary conditions for the lattice and random initial conditions $x_o^{(i)}$.

We build the scale-free lattice by means of a sequence of steps $s=0,1,2,\ldots s_{max}$, starting from an initial lattice with $N_0=11$ sites [Fig. 2(a)]. At each step s a new site is inserted in the lattice of size N_s, such that it is connected to ℓ randomly chosen sites. We observed that ℓ must be equal or greater than 2 in order to generate scale-free networks. According to the scale-free distribution, the connections occur preferentially with the more connected sites, which can be accomplished by using a different probability for each site $P_s^{(i)}=k_s^{(i)}/N_s$, where $k_s^{(i)}$ is the number of connections *per* site at the step s. The process is repeated until we achieve a desired lattice size N, which we choose as $N=230$ in the numerical simulations to be presented in this paper. After a number s_{max} of steps we have $k^{(i)}$ connections *per* site, corresponding to a probability $P^{(i)}=k^{(i)}/N$. Figure 2(b) shows a histogram for the number of sites with connectivity k, obtained through this procedure for $N=230$ sites. The numerical approximation to the (non-normalized) probability distribution function is shown to display the scale-free signature of a power-law scaling $k^{-\varpi}$ with a slope $\varpi=2.08$, which compares well with the experimental values reported in Ref. [10].

A scale-free coupled map lattice obtained from Eqs. (5) and (6) can be written also in the form

$$x_{n+1}^{(i)} = \frac{\alpha^{(i)}}{1+(x_n^{(i)})^2} + y_n^{(i)} + \frac{\epsilon}{k^{(i)}} \sum_{j=1}^{N} g_{ij} x_n^{(j)}, \tag{9}$$

$$y_{n+1}^{(i)} = y_n^{(i)} - \sigma^{(i)} x_n^{(i)} + \beta^{(i)}, \tag{10}$$

where g_{ij} are the elements of a $N\times N$ connectivity matrix, where $g_{ij}=1$ if the sites i and j are connected, and zero otherwise. Since the connectivity *per* site is different, each line of the matrix g_{ij} has a different number of 1's distributed through the columns, the remaining elements being padded with 0's. However, the connectivity matrix is symmetric ($g_{ij}=g_{ji}$) due to the process of construction of the scale-free lattice, i.e., the connectivity matrix evolves through a finite number of steps conserving its symmetry.

To conclude this section, we wish to emphasize that, in order for this coupled map lattice to exhibit a completely synchronized state,

$$x_n^{(1)} = x_n^{(2)} = \cdots = x_n^{(N)}, \quad y_n^{(1)} = y_n^{(2)} = \cdots = y_n^{(N)}, \qquad (11)$$

it is necessary that the latter be a possible solution of Eqs. (9) and (10). We remark that it would be also necessary that such a solution, if any, should be stable under infinitesimal perturbations along directions transversal to the state (11). However, since the parameters of the model (α, β, σ, and k) are different (and randomly chosen inside a given interval) for the coupled sites, we can rule out the possibility of having a completely synchronized state. There can be chaotic phase synchronization, however, as we will see in the next section.

IV. PHASE SYNCHRONIZATION OF BURSTING NEURONS

Even though we cannot have completely synchronized states for the coupled map lattice (9) and (10), this does not mean the absence of coherent behavior in the system. In Sec. II we have defined a phase for the bursting dynamics of an isolated neuron, in such a way that the chaotic spiking evolution in the fast time scale is modulated by a nearly regular oscillation in the slow time scale. We can thus look for a form of coherent behavior characterized by the near coincidence of the bursting phases for an assembly of connected neurons, which is identified as chaotic phase synchronization. The latter has been extensively investigated in a variety of physical and biological systems [40].

For just two coupled neurons, we could describe chaotic phase synchronization simply by stating that their phases be approximately equal, up to a given tolerance C: $|\varphi^{(1)} - \varphi^{(2)}| < C \ll 1$. In the case of a large number N of systems, however, other diagnostics of phase synchronization need to be used. One such indicator is the mean field of the lattice,

$$M = \frac{1}{N}\sum_{j=1}^{N} x_n^{(j)}. \qquad (12)$$

If the neurons are weakly coupled, for example, since they burst at different times in a noncoherent fashion, the mean field fluctuates irregularly with small amplitudes. On the other hand, if the neurons burst together synchronously a nonzero mean field is formed and M presents regular oscillations (due to the common rhythm) of comparatively large amplitude. Only the slow time scale dynamics becomes coherent as the neurons burst synchronously, and the fast time scale spiking remains incoherent and does not contribute to the mean field dynamics, which is kept close to a periodic regime [7].

If we consider an assembly of uncoupled neurons ($\epsilon=0$) with different values of the α parameter chosen within the interval $4.1<\alpha<4.4$ the mean field indeed has small-amplitude noisy fluctuations [Fig. 3(a)] indicating that the neurons are not bursting in phase, as can be seen by comparing the uncorrelated bursting activity of two selected neurons [Figs. 3(c) and 3(e)]. On the other hand, as long as the neurons are coupled in the scale-free lattice, for a sufficiently large coupling strength ϵ the mean field exhibits large-amplitude oscillations [Fig. 3(b)] since neurons burst at approximately the same time, in spite of their spiking evolution being poorly or not correlated at all [Figs. 3(d) and 3(f)]. Figure 4 shows the time evolution of the phases of these bursting neurons. While both maps present a monotonic increase of their phases with time, if they are uncoupled these evolutions are mutually independent since their phase difference grows with time and eventually becomes as large as the phases themselves. The phase difference is kept in a small value if the neurons are coupled in the network.

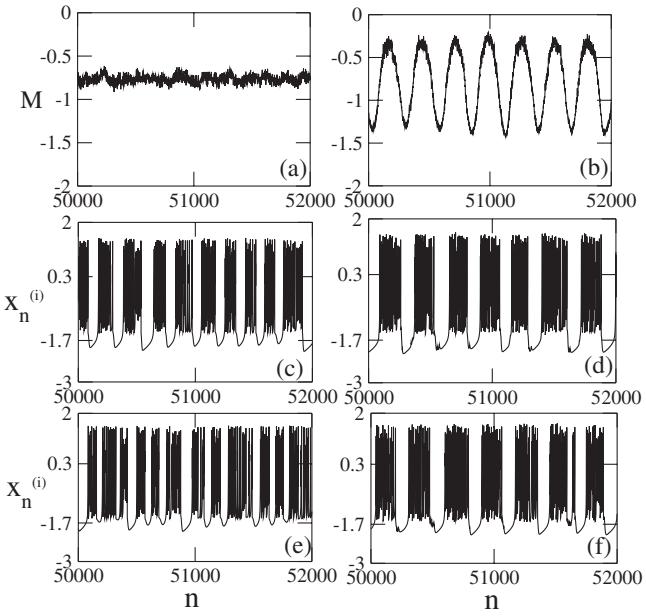

FIG. 3. Time evolution of the mean field for a scale-free lattice of Rulkov neurons with (a) $\epsilon=0$, and (b) $\epsilon=0.04$. Time evolution of the fast variable for a map with (c) $\alpha^{(i)}=4.1$ and (e) $\alpha^{(j)}=4.4$ for $\epsilon=0.0$ where bursting is uncorrelated. (d) and (f) are the respective situations for $\epsilon=0.04$, showing approximate synchronization of bursting.

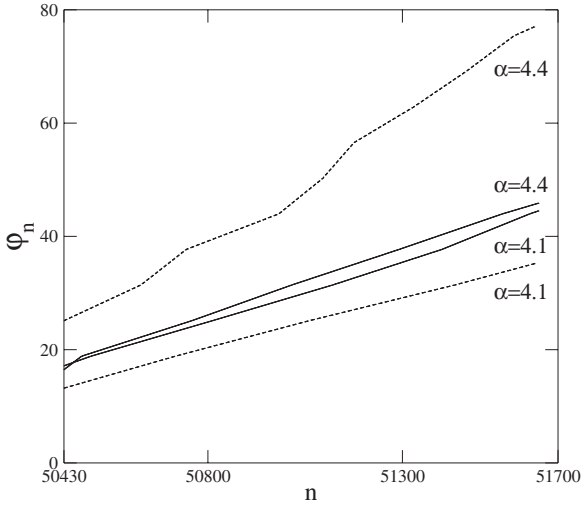

FIG. 4. Time evolution of the phase for two selected maps ($\alpha^{(i)}=4.1$ and $\alpha^{(j)}=4.4$) belonging to a scale-free lattice of Rulkov neurons with $\epsilon=0$ (dashed lines) and $\epsilon=0.04$ (full lines).

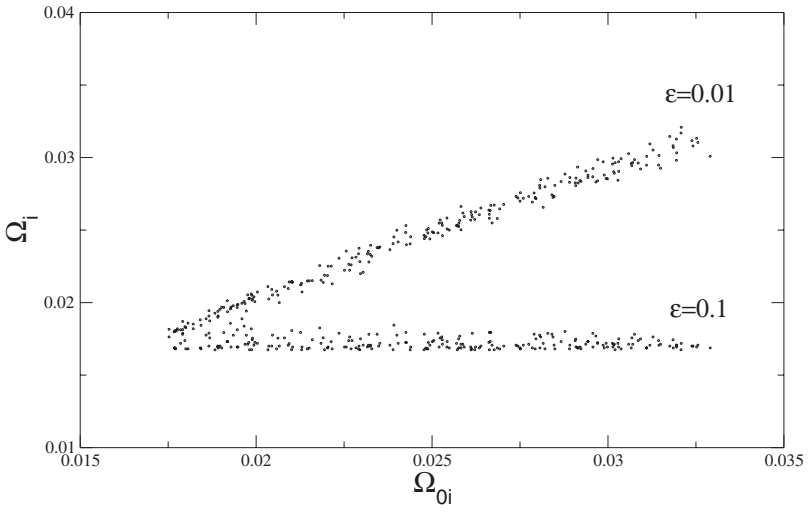

FIG. 5. Bursting frequency for the scale-free lattice vs the zero-coupling frequencies for two values of the coupling strength ϵ.

If the oscillator phases are synchronized, so are their time rates, also called bursting frequencies, hence we can characterize numerically synchronization of bursting by the existence of synchronization plateaus. We compare the frequency of the coupled neuron $\Omega^{(i)}$, given by Eq. (4), with the unperturbed frequencies observed for zero coupling, $\Omega_0^{(i)}$, the latter being expected to fluctuate randomly. If there is chaotic phase synchronization, a number of sites form a synchronization plateau with a constant value of $\Omega^{(i)}$ for many sites characterized by different values of $\Omega_0^{(i)}$ (not necessarily neighbors in the lattice, though).

The behavior of the bursting frequencies $\Omega^{(i)}$ is illustrated by Fig. 5, where we plotted them vs the zero-coupling frequencies $\Omega_0^{(i)}$ which, for the parameter values we adopted, take on values within the interval [0.0175,0.0330]. When the coupling strength is low enough there is no synchronization of bursting and we expect the frequencies to approach their zero-coupling limit. In fact they are distributed so as to have a linear trend $\Omega^{(i)} \approx \Omega_0^{(i)}$. Increasing the coupling strength indeed leads to phase and frequency synchronization of bursts, since the frequencies are distributed around a mean value of ~ 0.016 with a small dispersion coming from the imperfect character of the phase synchronized states.

We can also use, as a diagnostic of chaotic phase synchronization, the complex phase order parameter

$$z_n = R_n \exp(i\Phi_n) \equiv \frac{1}{N}\sum_{j=1}^{N} \exp(i\varphi_n^{(j)}), \tag{13}$$

where R_n and Φ_n are the amplitude and angle, respectively, of a centroid phase vector for a one-dimensional lattice with periodic boundary conditions. For uncoupled maps, we would expect patterns for which the bursting phases $\varphi_n^{(j)}$ are spatially uncorrelated such that their contribution to the result of the summation in Eq. (13) is typically small. In particular, for a uniform distribution of $\varphi_n^{(i)}$ the order parameter magnitude would be zero. On the other hand, in a completely phase synchronized state the order parameter magnitude rapidly tends to unity, indicating a coherent superposition of the phase vectors for all sites with the same amplitudes R_n at each time. The time averaged order parameter magnitude

$$\bar{R} = \lim_{T\to\infty} \frac{1}{T}\sum_{n=m}^{T} R_n, \tag{14}$$

where we have discarded the first $m-1$ transient map iterations, can be used to investigate the transition to phase synchronization of bursts as the coupling strength is varied, as illustrated by Fig. 6.

The scale-free lattice we have considered is obtained through a sequence of steps, beginning from a seed lattice of $N_0=11$ sites and adding randomly sites with ℓ connections for each step until reaching the final number of $N=230$ sites. We observed that a scale-free lattice with good synchronization properties is possible only for $\ell \geqslant 2$, since for $\ell=1$ the average order parameter cannot achieve values larger than 0.75 even if strong coupling is used. On the other hand, for $\ell=2$ and a coupling strong enough we have order parameter values fluctuating with time around approximately 0.8 [like the case for which $\epsilon=0.07$ in Fig. 7(a)]. As this coupling

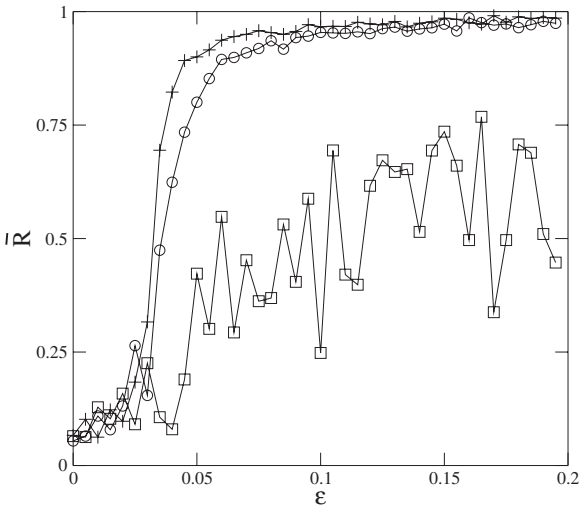

FIG. 6. Time-averaged order parameter as a function of the coupling strength ε for a scale-free lattice with $N=230$ and built with a different number of links *per* step: $\ell=1$ (squares), $\ell=2$ (circles), and $\ell=3$ (crosses).

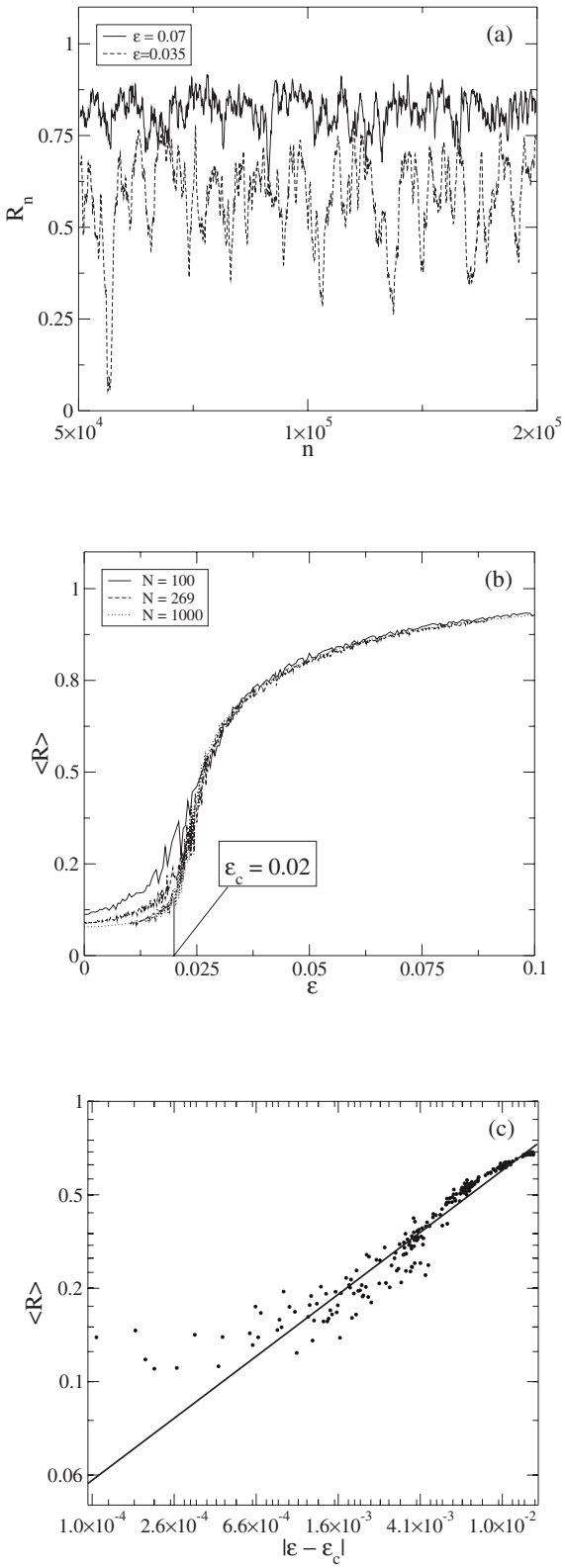

FIG. 7. (a) Time evolution of the order parameter magnitude for two values of the coupling strength. (b) Average order parameter magnitude as a function of ϵ for different lattice sizes. The critical value of $\epsilon_c=0.02$ results from an extrapolation to the thermodynamical limit. (c) Scaling behavior of the average order parameter magnitude near the critical point. The full line represents a least-squares fit giving a power law with exponent 0.5 (see text).

strength is decreased the phase synchronization of bursting becomes more imperfect, fluctuating around a smaller value of R and with more dispersion as well [as illustrated by the case of $\epsilon=0.035$ in Fig. 7(a)]. The minimum value of the mean order parameter $\langle R\rangle_{min}$ is obtained for zero coupling, and decreases as the lattice turns larger [Fig. 7(b)]. Supposing that $\langle R\rangle_{min}$ goes to a small (yet probably nonzero) limiting value as we take the thermodynamical limit ($N\to\infty$) we extrapolated the behavior illustrated by Fig. 7(b) for increasing lattice size and considered $\epsilon_c=0.02$ as an approximate value for the critical coupling strength.

In Ref. [7] the transition to chaotic phase synchronization of bursting was identified as a second-order phase transition. We have verified this claim in the case of a scale-free lattice by considering the behavior near criticality of the mean order parameter, as depicted by Fig. 7(c), where we obtained a power-law scaling which is analogous to the behavior observed in Kuramoto's model of mean field coupled phase oscillators [41],

$$\langle R\rangle \sim |\epsilon-\epsilon_c|^{\kappa}, \tag{15}$$

where a least squares fit leads to the exponent $\kappa=0.502\pm0.007$, which agrees with the exponent 1/2 characteristic of magnetic phase transition [42].

V. EXTERNAL PHASE SYNCHRONIZATION

In the previous section we demonstrated that neurons in a scale-free coupled lattice are able to synchronize their bursting activities, even though the chaotic spiking in the fast time scale remains uncorrelated. Once those neurons synchronize at a certain frequency, we can additionally investigate at what extent we are able to synchronize them with an external periodic signal. Such kind of external stimulation of brain has been extensively studied with respect to potential application to the control of pathological rhythms, since the synchronization of individual neurons is thought to play a key role in Parkinson's disease, essential tremor, and epilepsies [43]. This intervention is experimentally feasible by means of microelectrodes inserted into the impaired region of the brain and carrying a suitable electric signal [44].

In this case, however, rather than trying to synchronize the neurons with the external signal, one would wish to suppress those brain rhythms. Nevertheless, the latter problem belongs to the same category as the external synchronization of neurons with an external source, since one would like to know the parameter ranges for which phase synchronization occurs or does not occur. Rosenblum and Pikovsky have put forward this idea by using a delayed feedback control on a globally coupled neural oscillator network [27]. Ivanchenko *et al.* [7] have proposed the use of an additive periodic signal to a selected site of such a lattice, with amplitude d and frequency ω.

We have implemented numerically this external time-periodic intervention to the scale-free lattice studied in this work. An external harmonic signal is applied to a selected neuron in the following way:

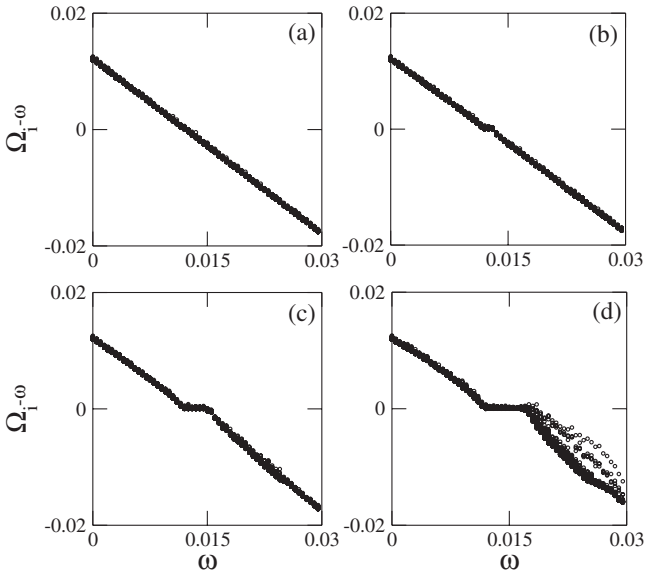

FIG. 8. Frequency mismatch of bursting neurons vs the external driving frequency for a scale-free lattice with $\epsilon=0.2$ and an a driving signal with amplitude (a) $d=0.05$, (b) $d=0.09$, (c) $d=0.15$, and (d) $d=0.20$.

$$x_{n+1}^{(1)} = \frac{\alpha^{(1)}}{1+(x_n^{(1)})^2} + y_n^{(1)} + \frac{\epsilon}{k^{(1)}} \sum_{j=1}^{N} g_{1j} x_n^{(j)} + d\,\sin(\omega n), \qquad (16)$$

where we have chosen the site $i=1$ with the largest number of connections; the remaining $N-1$ neurons remaining unchanged. In order to investigate the effect of this external source we have used coupling strength values for which the unperturbed lattice ($d=0$) exhibits bursting synchronization, their corresponding frequencies $\Omega^{(i)}$ locking approximately at a common value, as depicted in Fig. 5.

When the driving amplitude d is nonzero, we considered many situations for which the neurons synchronize at different common frequencies $\Omega^{(i)}$ within the range [0,0.03] and plotted in Fig. 8 the corresponding mismatches with the external signal frequency ω. If the signal amplitude is too low [Fig. 8(a)] the difference $\Omega^{(i)}-\omega$ vanishes for a particular value of ω, but for $d \gtrsim 0.09$ we obtain a narrow frequency locking interval around $\Omega=0.013$. The width of this locking interval, $\Delta\omega$, increases with the signal amplitude [Figs. 8(c) and 8(d)], in a situation akin to the Arnold tongue structure existing for periodically forced oscillators [45]. The wider the frequency-locking interval is, the more robust is the external driving with respect to imperfect parameter determination and noise, which is a question of considerable experimental importance.

The wide variety of connections *per* site in a scale-free lattice makes the choice of the site upon which the control is applied a key factor influencing the results. If one chooses a richly connected site the influence of the external control is more pronounced than for a poorly connected one. According to Fig. 9(a) the most connected site is the one with $i=1$, which has $k^{(1)}=17$ connections, whereas for most of the remaining sites this number is substantially less than 10. In order to evaluate the effectiveness of the connectivity $k^{(i)}$ we computed the width of the frequency-locking intervals for a fixed perturbation strength d and varying the lattice site upon which the control is applied [Fig. 9(b)]. Not by chance, the site $i=1$ has a frequency-locking interval almost three times wider than that obtained with most of the remaining sites. Since, in a "blind" experiment we cannot know in advance the connectivity of a site we should expect that, with reasonable probability, the frequency-locking interval is that exhibited by the most part of the poorly connected sites. One possible way to circumvent this problem would be to use more than one site to control at the same time (multiple pinnings) [7].

The widening of the frequency-locking intervals as we increase the amplitude of the driving signal, as observed in Fig. 8, seems to be limited by the intensity of the external signal, since for higher d the bursting frequencies are different from each other when the driving frequency is higher than the upper end of the frequency locking interval $\omega_c \approx 0.016$ [Fig. 8(d)], characterizing a kind of instability of the frequency-locked state for $d \gtrsim d_c=0.15$. A qualitative explanation for this instability is that, for a too large perturbation strength, the Arnold-like tongue overlaps with other ones and the chaotic output strongly depends on the initial condition we choose, which explains the diversity of values of $\Omega^{(i)}-\omega$ for large d depicted in Fig. 8(d).

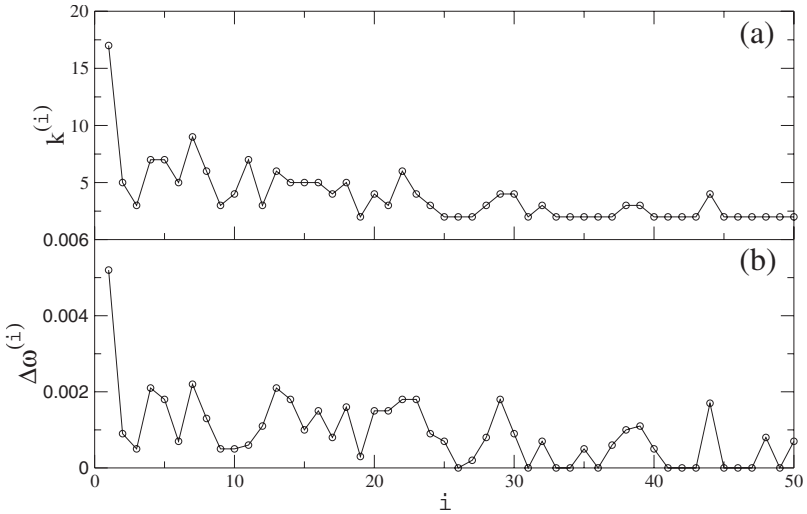

FIG. 9. (a) Connectivity per site of a scale-free lattice with $\epsilon=0.2$; (b) width of the frequency-locking interval vs lattice site for a driving signal with amplitude $d=0.20$.

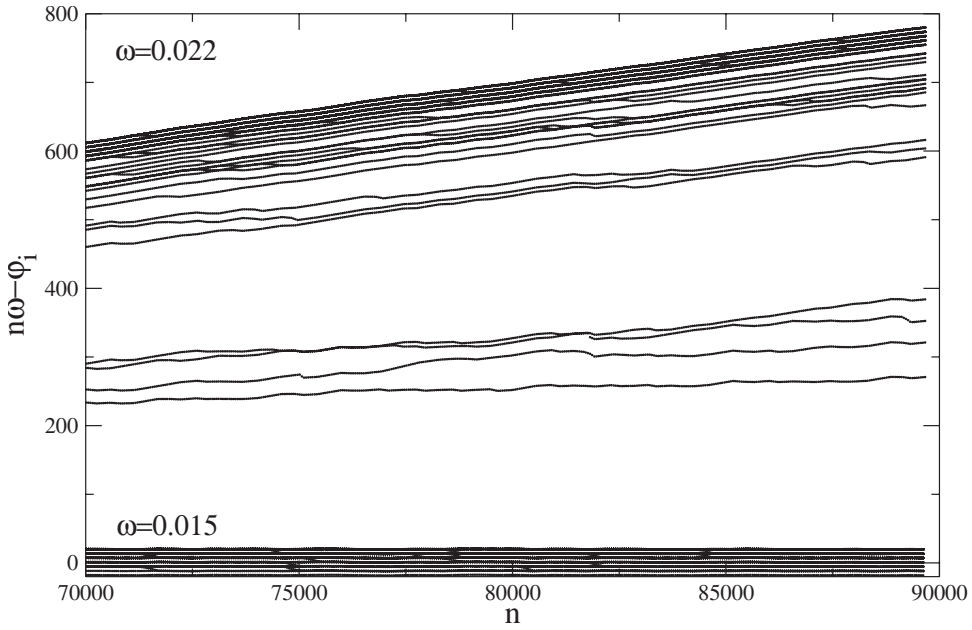

FIG. 10. Time evolution of the difference between the bursting and driving phases for two values of the driving frequency.

In order to investigate the effect of driving frequencies larger than the critical frequency $\omega_c \approx 0.016$ we have plotted in Fig. 10 the time evolution of the phase difference between the bursting phase and the driving phase $\phi \equiv \omega n$. For a precritical frequency $\omega \lesssim \omega_c$ this difference stays constant and very small for all neurons, so characterizing a frequency-locked state. If $\omega \gtrsim \omega_c$, by way of contrast, the phases begin to diffuse and the corresponding frequencies, which turn to be the corresponding average time rates, are different for each map.

There is an overall monotonic increase of the phase difference $\phi - \varphi^{(i)}$ with constant steps of variable width. This is the well-known effect of phase slips, and bears a general character, since it is related to the intermittent breakup of the phase synchronized state [46]. In this situation, the influence of the external signal is strong enough to steer the system out of the phase synchronized state (i.e., the frequency-locking interval) provoking a phase drift. The system eventually returns to the vicinity of the synchronized state, the corresponding laminar intervals having different durations. It would be desirable to avoid such intermittent episodes of nonsynchronization in practical implementations of this external control procedure.

VI. CONCLUSIONS

Motivated by recent experimental evidence [10] that the brain functional network has the scale-free property, in which the connectivity of the coupled units obeys a power-law scaling, we constructed a scale-free lattice, by adding randomly new sites to a seed lattice in such a way that richly connected sites are more likely to have new additions than poorly connected ones. The procedure we used resulted in an artificial scale-free network with a similar scaling law as that experimentally obtained by Chialvo and coworkers. The neuron dynamics was simulated by a two-dimensional map which presents two time scales in order to exhibit both spiking and bursting behaviors. Other more sophisticated models for neuron activity could be likewise used, but the essentials of the multiple time scale behavior are already present in the map we used.

We focused in this paper on collective effects emerging from the complex dynamics generated by such a coupled map lattice. Since complete synchronization is ruled out for our system of heterogeneous coupled units (as would be required in realistic models of brain networks), we investigated chaotic phase synchronization after defining a convenient phase for the bursting dynamics. We observed that the phases of different coupled maps can undergo similar evolution with time as the coupling strength increases, configuring a transition to chaotic phase synchronization. The existence of phase synchronized states enhances the information processing properties of the network, since information can be coded in the interphase intervals, such that clusters of similar neurons would act cooperatively in order to produce a coherent outcome. We characterized those collective effects using various numerical diagnostics, such as the analysis of plateaus of perturbed frequencies and a complex order parameter.

Following a recent proposal that external stimulation of brain areas is effective on controlling certain dynamical behaviors [27], we used a time-periodic external driving signal applied to a selected neuron from the scale-free network we investigate. We observed the appearance of frequency locking between the bursting and driving phases. The width of the frequency-locking interval increases with the driving amplitude up to a saturation due to chaotic evolution associated with the bursting dynamics. On the other hand, depending on the connectivity of the site, in a scale-free lattice widely different intervals can be obtained. In practice, when we do not have a prior knowledge of the connectivity we must expect a relatively low interval when picking up at random a neuron to control. In such a case multiple pinnings, applied to more than one neuron, would be necessary to obtain

frequency-locking intervals wide enough to be robust against imperfect parameter determination and noise. This seems to be a promising line of investigation we are currently pursuing using the coupled map lattice model presented in this paper.

ACKNOWLEDGMENTS

This work was made possible with help of CNPq, CAPES, and Fundação Araucária (Brazilian Government Agencies).

[1] M. F. Bear, B. W. Connors, and M. A. Paradiso, *Neuroscience: Exploring the Brain*, 2nd ed. (Lippincott Williams & Wilkins, Philadelphia, 2002).
[2] I. Belykh, E. de Lange, and M. Hasler, Phys. Rev. Lett. **94**, 188101 (2005).
[3] *Bursting: The Genesis of Rhythm in the Nervous System*, edited by S. Coombes and P. C. Bressloff (World Scientific, Singapore, 2005).
[4] J. L. Hindmarsch and R. M. Rose, Philos. Trans. R. Soc. London, Ser. B **221**, 87 (1984).
[5] D. Chialvo, Chaos, Solitons Fractals **5**, 461 (1995).
[6] N. F. Rulkov, Phys. Rev. Lett. **86**, 183 (2001).
[7] M. V. Ivanchenko, G. V. Osipov, V. D. Shalfeev, and J. Kurths, Phys. Rev. Lett. **93**, 134101 (2004).
[8] A. S. Pikovsky, M. G. Rosenblum, and J. Kurths, *Synchronization: A Universal Concept in Nonlinear Sciences* (Cambridge University Press, Cambridge, England, 2003).
[9] M. G. Rosenblum, A. S. Pikovsky, and J. Kurths, Phys. Rev. Lett. **76**, 1804 (1996).
[10] D. R. Chialvo, Physica A **340**, 756 (2004); O. Sporns, D. R. Chialvo, M. Kaiser, and C. C. Hilgetag, Trends Cogn. Sci. **8**, 418 (2004); V. M. Eguiluz, D. R. Chialvo, G. A. Cecchi, M. Baliki, and A. V. Apkarian, Phys. Rev. Lett. **94**, 018102 (2005).
[11] A.-L. Barabási and R. Albert, Science **286**, 509 (1999).
[12] R. Albert and A.-L. Barabási, Rev. Mod. Phys. **74**, 47 (2002); S. N. Dorogovtsev and J. F. F. Mendes, Adv. Phys. **51**, 1079 (2002).
[13] A.-L. Barabási, R. Albert, and H. Jeong, Physica A **281**, 21115 (2000); A. Broder, R. Kumar, F. Maghoul, P. Raghavan, S. Rajagopalan, R. Stata, A. Tomkins, and J. Wiener, Comput. Netw. **33**, 309 (2000); R. Pastor-Satorras, A. Vázquez, and A. Vespignani, Phys. Rev. Lett. **87**, 258701 (2001).
[14] M. Baiesi and M. Paczuski, Phys. Rev. E **69**, 066106 (2004).
[15] A. P. S. de Moura, Y.-C. Lai, and A. E. Motter, Phys. Rev. E **68**, 017102 (2003).
[16] R. Pastor-Satorras and A. Vespignani, Phys. Rev. Lett. **86**, 3200 (2001).
[17] F. Lijeros, C. R. Edling, L. A. N. Amaral, H. E. Stanley, and Y. Aberg, Nature (London) **411**, 907 (2001).
[18] S. Wuchty, Mol. Biol. Evol. **18**, 1694 (2001).
[19] H. Jeong, B. Tombor, R. Albert, Z. N. Oltvai, and A.-L. Barabási, Nature (London) **407**, 651 (2000); H. Jeong, S. Mason, A.-L. Barabási, and Z. N. Oltvai, *ibid.* **411**, 41 (2001); A.-L. Barabási and Z. N. Oltvai, Nat. Rev. Genet. **5**, 101 (2004).
[20] P. G. Lind, J. A. C. Gallas, and H. J. Herrmann, Phys. Rev. E **70**, 056207 (2004).
[21] Y. Moreno and A. F. Pacheco, Europhys. Lett. **68**, 603 (2004).
[22] C. A. S. Batista, A. M. Batista, S. E. de S. Pinto, R. L. Viana, S. R. Lopes, and I. L. Caldas, Physica A (to be published).
[23] C. Zhou and J. Kurths, Phys. Rev. Lett. **96**, 164102 (2006).
[24] J. R. Gibson, M. Beierfein, and B. W. Connors, Nature (London) **402**, 75 (1999).
[25] A. M. Thomson, Curr. Biol. **10**, R110 (2000).
[26] E. M. Izhikevich, Int. J. Bifurcation Chaos Appl. Sci. Eng. **10**, 1171 (2000).
[27] M. Rosenblum and A. Pikovsky, Phys. Rev. E **70**, 041904 (2004).
[28] M. Dhamala, V. K. Jirsa, and M. Ding, Phys. Rev. Lett. **92**, 028101 (2004).
[29] N. F. Rulkov, Phys. Rev. E **65**, 041922 (2002); N. F. Rulkov, I. Timofeev, and M. Bazhenov, J. Comput. Neurosci. **17**, 203 (2004).
[30] P. Dayan and L. F. Abbott, *Theoretical Neuroscience: Computational and Mathematical Modeling of Neural Systems* (MIT Press, Cambridge MA, 2001).
[31] A. F. Rozenfeld, R. Cohen, D. ben-Avraham, and S. Havlin, Phys. Rev. Lett. **89**, 218701 (2002).
[32] K. Kaneko, in *Theory and Applications of Coupled Map Lattices*, edited by K. Kaneko (Wiley, Chichester, 1993).
[33] H. Nozawa, Chaos **2**, 377 (1992); S. Raghavachari and J. A. Glazier, Phys. Rev. Lett. **74**, 3297 (1995); S. Ishii and M. Sato, Physica D **121**, 344 (1998).
[34] T. B. Achacoso and W. S. Yamamoto, *AY's Neuroanatomy of C. elegans for Computation* (CRC Press, Boca Raton, FL, 1992).
[35] J. W. Scannell and M. P. Young, Curr. Biol. **3**, 191 (1993).
[36] O. Sporns, in *Neuroscience Databases: A Practical Guide*, edited by R. Kotter (Kluwer Publishers, Boston, MA, 2002), p. 169.
[37] D. J. Watts and S. H. Strogatz, Nature (London) **393**, 440 (1998).
[38] M. E. J. Newman and D. J. Watts, Phys. Lett. A **263**, 341 (1999); Phys. Rev. E **60**, 7332 (1999).
[39] C. Zhou, L. Zemanová, G. Zamora, C. C. Hilgetag, and J. Kurths, Phys. Rev. Lett. **97**, 238103 (2006).
[40] *Synchronization: Theory and Application*, edited by A. Pikovsky and Yu. Maistrenko (Kluwer, Dordrecht, 2003).
[41] J. A. Acebrón, L. L. Bonilla, C. D. P. Vicente, F. Ritort, and R. Spigler, Rev. Mod. Phys. **77**, 135 (2005).
[42] J. M. Yeomans, *Statistical Mechanics of Phase Transitions* (Oxford University Press, Oxford, 1992).
[43] *Epilepsy as a Dynamic Disease*, edited by J. Milton and P. Jung (Springer-Verlag, Berlin, 2003).
[44] A. Behabid *et al.*, Lancet **337**, 403 (1991).
[45] A. S. Pikovsky, M. G. Rosenblum, G. Osipov, and J. Kurths, Physica D **104**, 219 (1997).
[46] Z. Zheng, Gang Hu, and Bambi Hu, Phys. Rev. Lett. **81**, 5318 (1998).